Journal of the Mechanical Behavior of Biomedical Materials 77 (2018) 551–556

Contents lists available at ScienceDirect

Journal of the Mechanical Behavior of Biomedical Materials

journal homepage: www.elsevier.com/locate/jmbbm

Effects of non-enzymatic glycation on the micro- and nano-mechanics of articular cartilage

Parisa R. Moshtagh[a,b,*], Nicoline M. Korthagen[a,d], Mattie H.P. van Rijen[a], Rene M. Castelein[a], Amir A. Zadpoor[b], Harrie Weinans[a,b,c]

[a] Department of Orthopaedics, University Medical Center Utrecht, Utrecht, The Netherlands
[b] Faculty of Mechanical, Maritime, and Materials Engineering, Delft University of Technology (TU Delft), Mekelweg 2, Delft 2628 CD, The Netherlands
[c] Department of Rheumatology, University Medical Center Utrecht, Utrecht, The Netherlands
[d] Department of Equine Sciences, Faculty of Veterinary Medicine, Utrecht University, Utrecht, The Netherlands

ARTICLE INFO

Keywords:
Articular cartilage
Advanced glycation
Nano-stiffness
Micro-stiffness

ABSTRACT

The mechanical properties of articular cartilage depend on the quality of its matrix, which consists of collagens and glycosaminoglycans (GAGs). The accumulation of advanced glycation end products (AGEs) can greatly affect the mechanics of cartilage. In the current study, we simulated the accumulation of AGEs by using L-threose to cross-link collagen molecules in the cartilage matrix (in vitro). The resulting changes in the mechanical properties (stiffness) of cartilage are then measured both at the micrometer-scale (using micro-indenter) and nanometer-scale (using indentation-type atomic force microscopy). Non-enzymatic cross-linking within the cartilage matrix was confirmed by the browning of L-threose-treated samples. We observed > 3 times increase in the micro-scale stiffness and up to 12-fold increase in the nano-scale stiffness of the glycated cartilage in the peak pertaining to the collagen fibers, which is caused by cartilage network embrittlement. At the molecular level, we found that besides the collagen component, the glycation process also influenced the GAG macromolecules. Comparing cartilage samples before and after L-threose treatment revealed that artificially induced-AGEs also decelerate in vitro degradation (likely via matrix metalloproteinases), observed at both micro- and nano-scales. The combined observations suggest that non-enzymatic glycation may play multiple roles in mechanochemical functioning of articular cartilage.

1. Introduction

Osteoarthritis (OA) is categorized as a chronic and complicated degenerative disorder of the joints in which the natural turnover of glycosaminoglycans (GAGs) in articular cartilage is disrupted (Ghosh and Smith, 2002). Irreversible structural damage is mainly detectable in the progressed stages of OA at tissue level, while early degradations are initiated at a small molecular-scale from the early stage OA (Stolz et al., 2009; Chu et al., 2012). Among different layers of cartilage multi-zonal structure, the superficial layer is the first affected zone under degenerative conditions (Sophia Fox et al., 2009). This underscores the importance of detecting the molecular-scale changes of the cartilage surface layer. Aging is considered one of the major risk factors of OA as age-related accumulation of advanced glycation end products (AGEs) affects the synthesis and degradation of the collagen matrix (Saudek and Kay, 2003). AGEs are the result of a non-enzymatic reaction between amino acids (mainly lysine and arginine) and reducing sugars (e.g. threose) (Chen et al., 2002). The fact that the enhancement of AGEs accumulation makes the cartilage matrix stiffer and prone to fatigue failure is well described and is thought to be the result of increased collagen cross-linking (Verzijl et al., 2002). Since the biomechanical function of articular cartilage is under the control of chondrocytes, AGEs-related modifications may vary the chondrocytes' metabolism and alter the normal tissue turnover which eventually predisposes the cartilage tissue to OA (DeGroot et al., 2001).

Understanding the effects of AGEs on the cartilage matrix requires insight into how the biomechanical responses of various cartilage components are affected by AGEs. There is, however, not much data available in the literature as to how glycation influences the micro- and nano-mechanics of the cartilage (constituents). The overall aim of this study is to improve understanding of the effect of non-enzymatic glycation at both micro- and molecular levels in order to track the effect of AGEs on each cartilage component. In this study, we simulated the aging effect in rat knee cartilage using L-threose (in vitro). L-threose is a

* Correspondence to: Department of Orthopaedics, UMC Utrecht, Uppsalalaan 8, PO Box 85500, 3508 GA, 3584 CT Utrecht, The Netherlands.
E-mail addresses: p.rahnamaymoshtagh@umcutrecht.nl (P.R. Moshtagh), n.m.korthagen@uu.nl (N.M. Korthagen), M.Rijen@umcutrecht.nl (M.H.P. van Rijen), r.m.castelein@umcutrecht.nl (R.M. Castelein), a.a.zadpoor@tudelft.nl (A.A. Zadpoor), h.h.weinans@umcutrecht.nl (H. Weinans).

http://dx.doi.org/10.1016/j.jmbbm.2017.09.035
Received 27 April 2017; Received in revised form 16 September 2017; Accepted 27 September 2017
Available online 30 September 2017
1751-6161/

highly reactive carbohydrate that interacts with the cartilage matrix and increases the cross-linking of collagen, resulting in marked brownish color change (Saudek and Kay, 2003). We detected the resulting mechanical changes in both cartilage tissue (i.e. micro-scale) and the molecular constituents (i.e. nano-scale) respectively using micro-indentation and indentation-type atomic force microscopy.

2. Materials and methods

2.1. Sample harvesting and cross-linking

Intact knee joints were obtained from six 12-week-old male rats (Harlan Laboratories, Horst, Germany). Cartilage samples with underlying bone (~ 5 mm) were taken from the left (as control) and right (as test/crosslinking induced) femoral condyles of the same rat joint and stored at −20 °C. In order to induce cross-linking, the test cartilage was incubated with a solution of 100 mM L-threose (Sigma-Aldrich, Zwijndrecht, the Netherlands) in phosphate buffer solution (PBS, Gibco, UK) for 7 days at 37 °C, while the control cartilage was incubated in PBS only. Both solutions contained protease inhibitors (complete, Roche, Mannheim, Germany).

2.2. Biomechanical testing

2.2.1. Micro-scale indentation

Micro-indentations were performed on both test and control samples before (at day 0) and after the incubation (at day 7) using a microindenter machine (Piuma, The Netherlands) with a controller (Optics, The Netherlands) and a spherical indenter (radius: 48 μm, cantilever stiffness: 65.7 N/m). The Piuma indenter is referred to as a nanoindenter, but in fact this is not a correct representation as it yields micro-scale mechanical properties of the material. The applied indentation protocol was composed of a loading phase for 1 s at 18 μm indentation depth, which was held for 7 additional seconds, and then an unloading phase for 20 s. The actual indentation displacement is always lower than selected in the indentation profile, because the indentation depth that is selected is a combination of the cantilever deflection and the desired depth of indentation across the cartilage thickness (Moshtagh et al., 2016a). Before starting the experiments, signal calibration was performed and the geometrical factors of the probes were calibrated. Indentation measurements were done at a 9 × 9 grid within a region around 500 × 500 μm^2 (65 μm distance between each point, $n = 81$) at the central portion of the rat lateral femoral condyle (n = 5). The effective elastic modulus was calculated based on the Oliver-Pharr theory using the unloading force-displacement curves (Eq. (1)) (Oliver, 1992).

$$E_r = \frac{\frac{dp}{dh}}{2r^{1/2}\sqrt{h_{\max} - h_{final}}} \quad (1)$$

where P is the load, h is the displacement (indentation) and $\frac{dp}{dh}$ represents the slope of the initial part of the unloading curve in the load-displacement curve, r is the indenter radius, $h_{\max}$ and h_{final} are respectively maximum indentation and final unloading depths, and E_r is the effective elastic modulus. See Moshtagh et al. (2016a) for a more detailed description of this test.

In order to compare the mechanical properties measured at micro-scale, a one-way ANOVA followed by post-hoc analysis was performed using MATLAB with $p < 0.05$ as the statistical significance threshold.

2.2.2. Nano-scale indentation

Indentation-type atomic force microscopy (IT-AFM) was performed using a nanoscope controller (Bruker, Dimension V, Japan) with a standard fluid cell (Bruker) to obtain the indentation-based force-displacement curves. A nano-scale pyramidal tip (radius: 15 nm, cantilever spring constant: 0.06 N/m) (Nano and More, Germany) was utilized. The actual value of the cantilever spring constant was determined using the thermal tune method (Notbohm et al., 2011). Indentations were performed at day 0 and day 7 on the left (control) and right (treated) femoral condyle of only one animal, due to time constraints. Around 800 measurements were done at a 3 Hz frequency corresponding with an indentation rate of 3 μm/s and a depth of 500 nm (Moshtagh et al., 2016b). A Poisson ratio of 0.5 was adopted in accordance with the incompressibility assumption (Jin and Lewis, 2004). The Young's modulus was calculated using the Nanoscope analysis software (Bruker, version 1.4) based on the Sneddon's indentation theory (Eq. (2)) (Oliver, 1992). The histogram of the measured stiffness values (converted to probability density function) was analyzed using the four-component finite Gaussian mixture model (Zadpoor, 2015), which fits a weighted sum of multiple Gaussian distributions to the obtained raw data (Eq. (3)).

$$P = \frac{\pi \tan\varphi}{2\gamma^2}\frac{E}{1-\nu^2}h^2 \quad (2)$$

In the above equation, φ is the half angle of the cone, ν is the Poisson's ratio, and $\gamma = \pi/2$.

$$f(x) = \sum_{i=1}^{m} w_i N(\mu_i, \sigma_i) \quad (3)$$

where $f(x)$ is the probability distribution function and $N(\mu_i,\sigma_i)$ is the Gaussian probability. The mean, standard deviation, and weighting factor of each constituent (i) are respectively denoted by μ_i, σ_i, and w_i.

2.3. Histological examination

Knee joints were fixed in formaldehyde (4%, Klinipath, The Netherlands) for 2 days. Afterwards, the samples were decalcified with EDTA solution (12.5%, VWR, Belgium) for 21 days. They were then processed by means of graded ethanol steps to xylene, infiltrated and embedded in paraffin. Tissue sections with 5 μm thickness were sliced perpendicular to the cartilage surface using a microtome (Thermo scientific Micron HM 340E, Germany). Safranin-O staining with a fast green was used to stain the microscopic slides of the knee joints. They were then visualized using a light microscope (Olympus BX51, Japan).

3. Results

There were clear differences in the surface colors between the samples and the L-threose treated specimens became yellow-brown after 7 days of sugar incubation (Fig. 1a). More than 3-fold changes in the cartilage micro-stiffness before and after L-threose incubation were detected by micro-indentation (Table 1, control at day 7 vs. test at day 7). Comparing micro-scale data before and after incubation, shows relatively 2-fold decrease in the effective elastic modulus for the control (left) knees and 2-fold increase for L-threose treated right knees (test, Table 1). Although we observed variations over each sample (Fig. 1b), the difference between the average modulus of controls between day 0 and 7 was −55.4 ± 14.1%, while the difference between test samples before (day 0) and after sugar incubation (day 7) was +92.8 ± 95.1%. The micro-scale modulus of the L-threose-treated group (at day 7) was significantly different from their initial value (at day 0) as well as from the controls (only with PBS treated) at day 7 ($p = 0.002$). The actual indentation depths for control and test samples were respectively between 3.5–9 μm and 1.5–6 μm. Despite a large spatial variability of the modulus across the cartilage surface layer, quite similar (average) micro-stiffness with less than 18% changes between left and right knee joints for each rat at day 0 was observed (Fig. 1b). This indicates that applying a large number of indentations tests in accordance with the previously defined guidelines (Moshtagh et al., 2016a), indeed reduces the impact of intrinsic topographic variation.

For the nanoindentation using AFM, the Gaussian mixture model

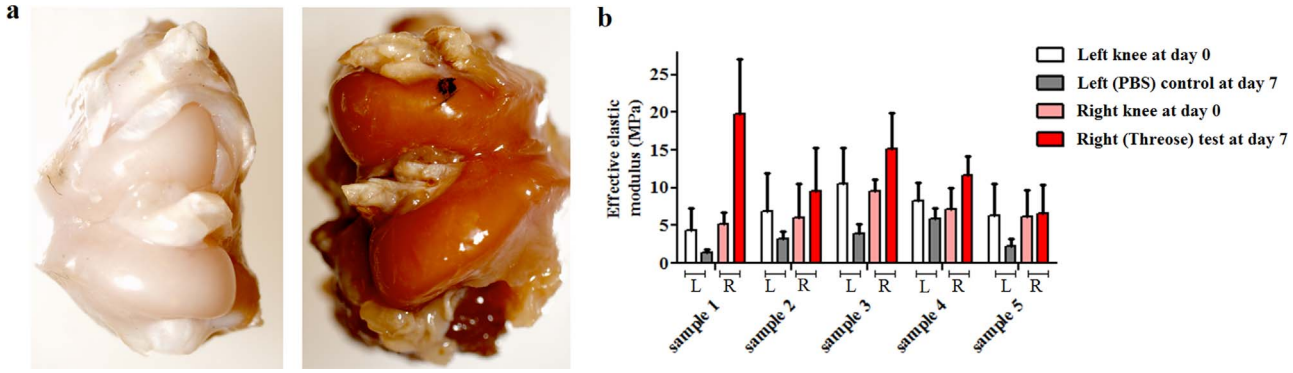

Fig. 1. (a) Femoral condyles after 7 days incubation with (Left) PBS as control, (Right) L-threose as test (b) Effective elastic modulus measured by micro-indenter at the micrometer-scale on the left (PBS control, L) and right (L-threose treated, R) femoral condyles; left knee at day 0 (white), left (PBS) control at day 7 (gray), right knee at day 0 (pink), and right (L-threose) test at day 7 (red), (b). (For interpretation of the references to color in this figure legend, the reader is referred to the web version of this article.)

Table 1
Average and standard deviation of the effective elastic modulus at micro-scale.

Sample name (n = 5)	*Effective elastic modulus (MPa) (mean ± SD)*
Left knee at day 0	7.26 ± 4.41
Left (PBS) control at day 7	3.35 ± 1.86
Right knee at day 0	6.41 ± 3.63
Right (Threose) test at day 7	12.16 ± 6.55

was fitted to the stiffness histogram to determine their peaks and the associated weighting factors (Table 2, Fig. 2). The optimum number of mixture components (at least four) was determined by applying statistical criteria described previously (Zadpoor, 2015) and by considering obtained weighing factors (Table 2). The nano-scale data detected remarkable changes in the modulus of each component of the cartilage tissue both as a consequence of time (control at 0 and 7 days) and L-threose (test at 0 and 7 days). When comparing control sample at day 0 and 7 (Fig. 2a, b), the modulus numbers markedly decreased in all four peaks by approximately 70–90%. However, after 7 days L-threose incubation (test sample at day 0 versus day 7; Fig. 2c, d), the first peak showed about 55% increase in the modulus and the third peak illustrated relatively no change (−10%). The second and fourth peaks showed about 40% decrease. Comparing the overall nano-scale modulus between the left (PBS treated control) knee and right (L-threose treated) knee after 7 days incubation, indicates a huge increase in all four peaks up to 12-fold was caused by L-threose (Fig. 2b, d).

Different layers of cartilage tissue with underlying subchondral bone are shown in Fig. 3. In the histological observation of the safranin-O slides, both groups showed lower proteoglycan concentration after 7 days incubation as compared to day 0 (Fig. 3a). In addition, it seems that the L-threose treated specimens (test) have slightly higher GAG content compared to the control group (both after 7 days of incubation) (Fig. 3b, c).

4. Discussion

In this study, we examined the effects of L-threose cross-linking on the mechanical stiffness properties of the cartilage matrix at nanometer and micrometer scales. We found > 3-fold rise in tissue stiffness at the micro-scale as shown by a significantly higher elastic modulus in the threose treated specimen compared to the control. According to previous finings (McGann et al., 2014; Kokkonen et al., 2011), an increased elastic modulus in L-threose or ribose-treated cartilage, indicates that enhanced levels of cross-linked collagens results in a stiff matrix causing chondrocytes to potentially feel less deformation under loading. This could have significant effects on the chondrocytes' responses and likely results in impaired repair responses (Chen et al., 2002; Verzijl et al., 2002; DeGroot et al., 2001). In addition, as opposed to the control samples that exhibited a clear reduction in the micro-scale effective elastic modulus after 7 days PBS incubation, due to normal degradation, test samples generally presented a significantly higher modulus (Table 1). Indicating that incubation with L-threose may protect cartilage from degradation, at least in vitro.

At the nano-scale, we detected an effect of cross-linking on both the collagen and glycosaminoglycan components separately. Comparing the range of stiffness with the literature (Moshtagh et al., 2016b), the third peak is most likely related to the nano-stiffness of the collagen fibers. As a result of L-threose cross-linking, the collagen component showed relatively unaffected nano-stiffness (1722 kPa vs. 1542 kPa) while it was reduced from 805 kPa to 130 kPa after 7 days PBS-incubation. This confirmed that L-threose treatment also results in higher collagen modulus at the nano-scale, which might speculate that the normal degradation procedure can be influenced by the threose treatment. Excessive collagen cross-linking through sugar-based treatment is not the only reason for the differences observed in the cartilage mechanical response. As a consequence of the cross-linking reactions, the density of negative charges increases while the positive charge of the collagen molecules declines (Jin and Lewis, 2004). Therefore, the net negative charge density is enhanced resulting in higher osmotic pressure and swelling of the cartilage due to high tonicity, and consequently, a greater elastic modulus (DeGroot et al., 2001; Kokkonen et al., 2011). Further investigation at the molecular level can provide useful information which cannot be directly determined using indentation analysis focused in the current study.

Table 2
Maximum likelihood estimates of the parameters of the Gaussian finite mixture models when 4 Gaussian components were used.

Sample name	μ_1 (kPa)	μ_2 (kPa)	μ_3 (kPa)	μ_4 (kPa)	σ_1 (kPa)	σ_2 (kPa)	σ_3 (kPa)	σ_4 (kPa)	w_1	w_2	w_3	w_4
L0	94.3	288.1	805.1	2022.4	20.3	124.7	358.1	968.8	0.16	0.47	0.28	0.09
C7	29.0	50.8	130.4	258.8	7.1	8.2	15.2	53.1	0.40	0.24	0.03	0.32
R0	96.6	669.6	1721.7	3734.3	20.8	261.1	660.6	1397.3	0.16	0.54	0.27	0.04
T7	150.3	373.6	1541.5	2283.2	56.6	14.1	310.8	1511.0	0.73	0.09	0.13	0.05

Left knee at day 0: L0, Left (PBS treated) control at day 7: C7, Right knee at day 0: R0, Right (Threose treated) test at day 7: T7, μ_i: Mean; σ_i: Standard deviation; w_i: Weighting factor of every constituent.

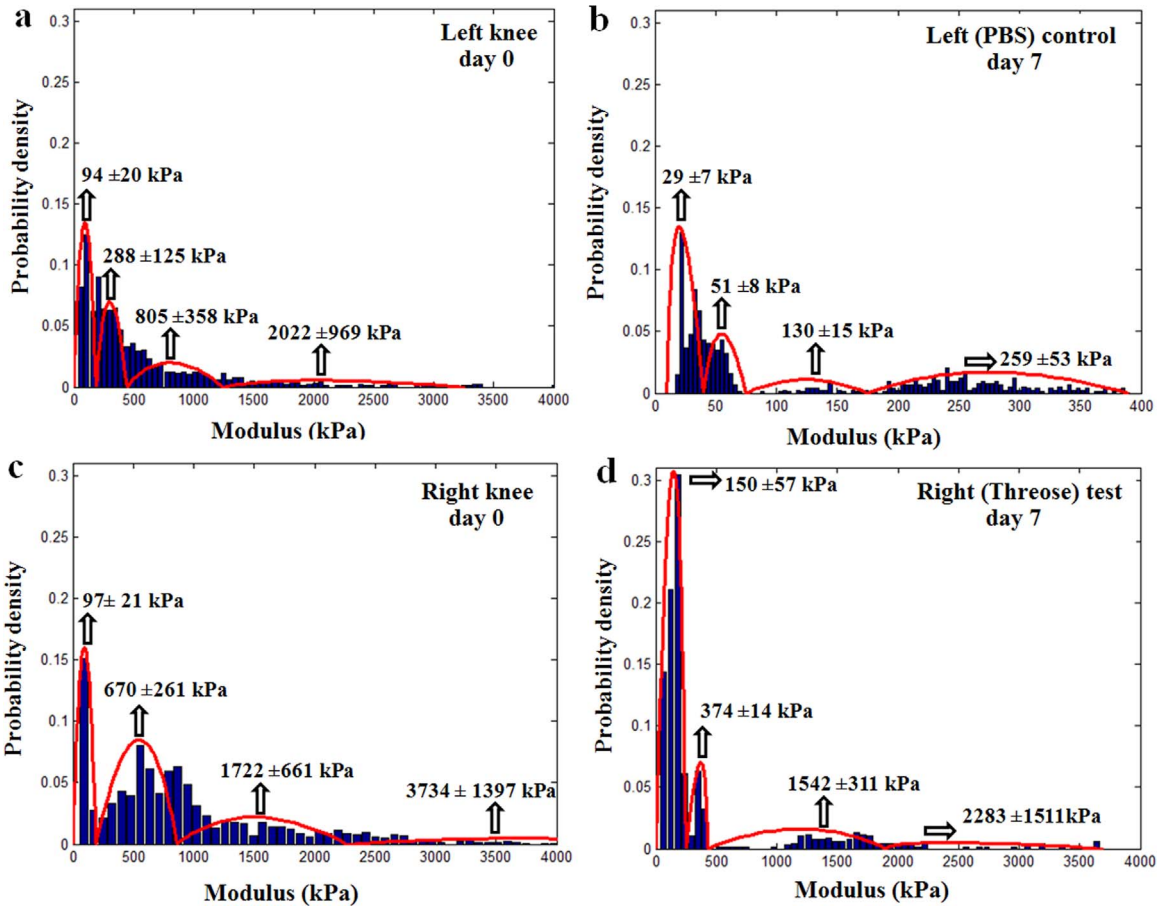

Fig. 2. The probability density distribution of the measured elastic modulus values via IT-AFM at the nano-scale on the left (PBS control) and right (L-threose treated) femoral condyles. (a) left knee at day 0, (b) left (PBS) control at day 7, (c) right knee at day 0, and (d) right (L-threose) test at day 7. In order to clearly show all different regions in the control sample (PBS-treated) after 7 days incubation, the figure legends in subfigure (b) is 10 times less than the other subfigures.

The peak with lower stiffness in the nano-scale bimodal modulus distribution of articular cartilage (first peak) is probably related to the stiffness of GAGs (Moshtagh et al., 2016b; Zadpoor, 2015; Loparic et al., 2010). By comparing the stiffness of the first and third peaks, it can be concluded that besides the well-known effect of AGEs on the cross-linking density of collagen fibers, it also has an influence on the polysaccharide chains. Similarly, measuring the shear equilibrium modulus of articular cartilage obtained from calf knee joints indicated that non-enzymatic glycation not only affects the collagen fibers but it likely reacts with the proteoglycans chains as well (Kerin et al., 2001). Moreover, the resulting increase in the net quantity of negative charge due to the glycation reaction together with additional cross-linking effects on proteoglycans chains (Kokkonen et al., 2011), indicate effects of AGEs on the diffusivity of solutes in the cartilage, especially in the surface layer (Leddy and Guliak, 2008).

Additionally, our results indicate that the softening effect of degradation is counteracted by threose, resulting in a smaller difference in the nano-scale modulus distribution of the collagens between 0 and 7 days in the test sample versus control (Fig. 2) (DeGroot et al., 2001). The nano-scale modulus of the second and forth peaks were also less affected after L-threose incubation than the control knee. A similar trend was observed on the effective elastic modulus changes at micro-scale (Fig. 1b). DeGroot et al. (2001) demonstrated that AGEs-induced articular cartilage (using a mixture of ribose and threose) was less susceptible to matrix metalloproteinase (MMP) degradation damage when they were exposed to the synovial fluid of patients with elevated amount of MMPs. It should be noted that the surface layer of rat articular cartilage shows highly location-dependent behavior in the mechanical properties (Moshtagh et al., 2016a), which prevents us from precisely distinguishing the small variations in the second and fourth peaks of the stiffness histogram measured by IT-AFM.

Histological staining shows variation in proteoglycan concentrations across the cartilage, some intrinsic spatial distribution especially in the superficial layer, and spatially variable cell death. Interestingly, proteoglycan content was slightly higher in the L-threose treated samples and cell death seems less pronounced indicating that GAG loss is not responsible for the large change in mechanical properties that is observed.

There are some limitations along with this study that need to be addressed: first, despite significant role of the cartilage surface layer focused in the current study, it is also very important to capture the mechanical response across the different cartilage zones. The mechanical response of bulk cartilage is likely to be different from the superficial zone (Tomkoria et al., 2004). Second, in order to obtain the biomechanics of cartilage considering its poroelastic nature, advanced analytical solutions need to be applied. Third, although mixture model can accurately predict the mechanical response of the individual component of cartilage, it also contains some level of uncertainties. For instance, even though the optimum number of peaks is chosen based on statistical criteria (Zadpoor, 2015), better understanding of the biomechanics of individual constitutes of articular cartilage, including the influence of dead cells as well as pericellular matrix, may yield in a different number of components (Darling et al., 2010). Finite Gaussian mixture model is assumed a Gaussian distribution for each probability distribution which is not necessarily true (Zadpoor, 2015). Furthermore, applying specific indentation protocol, besides using specific analytical methods might overlook the real behavior of cartilage tissue (Rauker et al., 2014).

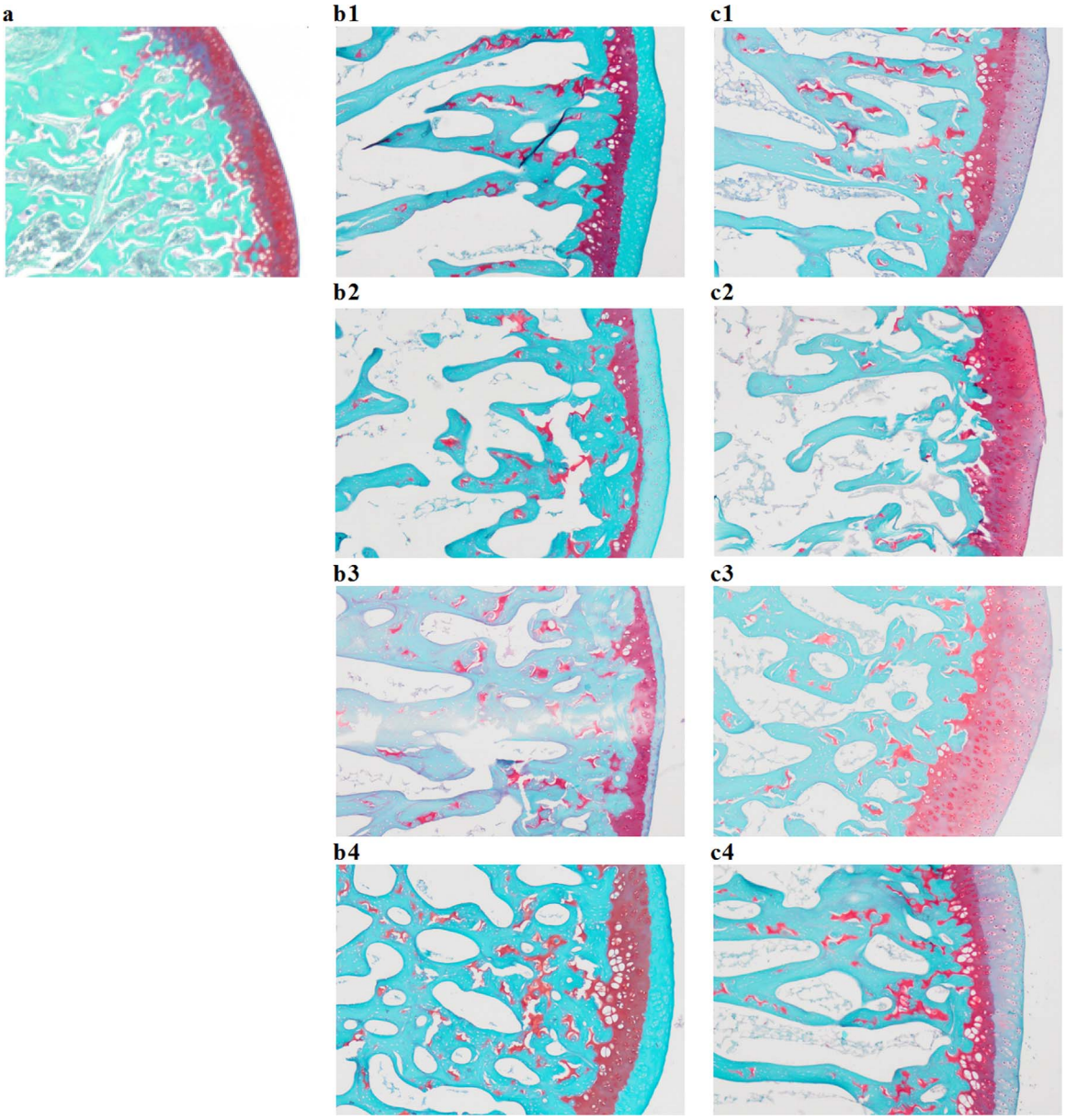

Fig. 3. Histology of cartilage specimens stained by Safranin-O. (a) knee joint at day 0, (b) left (PBS) controls at day 7, (c) right (L-threose) tests at day 7.

5. Conclusions

In conclusion, the current research investigates both tissue and molecular level changes in the cartilage stiffness as a result of non-enzymatic glycation. To the best of our knowledge, this is the first study that represents the nano-scale mechanical response of each component of sugar-treated articular cartilage, thereby providing mechanical stiffness information related to proteoglycans and collagen fibers. L-threose cross-linking of rat femoral condyles for 7 days incubation at 100 mM L-threose concentration leads to a 3–4 fold increase of stiffness. Furthermore, the data clearly demonstrates that L-threose cross-linking prevents normal (in vitro) degradation, indicating multiple roles of non-enzymatic glycation in the mechano-chemical functioning of articular cartilage. The overall changes in the charge distribution of the collagen molecules as well as a different conformation of cartilage macro-molecules as a consequence of AGEs may contribute to the observed prevention effects. Preliminary results show considerable AGEs-associated changes on the nano- and micro scales stiffness of the rat knee joint, and further analysis is needed to establish the significance of these finding.

Acknowledgement

We would like to acknowledge Dutch Arthritis Foundation (Reumafonds, 13-3-406 and LLP22) for its financial support and Kavli Nanolab group for their hospitality during the experiments.**Conflict of interest**

The authors of this research have no conflicts of interest to report concerning this article.

References

Chen, A.C., Temple, M.M., Ng, D.M., Verzijl, N., DeGroot, J., TeKoppele, J.M., et al., 2002. Induction of advanced glycation end products and alterations of the tensile properties of articular cartilage. Arthritis Rheum. 46 (12), 3212–3217.

Chu, C.R., Williams, A.A., Coyle, C.H., Bowers, M.E., 2012. Early diagnosis to enable early treatment of pre-osteoarthritis. Arthritis Res. Ther. 14 (3), 212.

Darling, E.M., Wilusz, R.E., Bolognesi, M.P., Zauscher, S., Guilak, F., 2010. Spatial mapping of the biomechanical properties of the pericellular matrix of articular

cartilage measured in situ via atomic force microscopy. Biophys. J. 98 (12), 2848–2856.
DeGroot, J., Verzijl, N., Wenting-Van Wijk, M.J., Bank, R.A., Lafeber, F.P., Bijlsma, J.W., et al., 2001. Age-related decrease in susceptibility of human articular cartilage to matrix metalloproteinase-mediated degradation: the role of advanced glycation end products. Arthritis Rheum. 44 (11), 2562–2571.
Ghosh, P., Smith, M., 2002. Osteoarthritis, genetic and molecular mechanisms. Biogerontology 3 (1–2), 85–88.
Jin, H., Lewis, J.L., 2004. Determination of Poisson's ratio of articular cartilage by indentation using different-sized indenters. J. Biomech. Eng. 126 (2), 138–145.
Kerin, A., Huang, G., Verzijl, N., DeGroot, J., TeKoppele, J., Grodzinsky, A., 2001. The effect of non-enzymatic glycation on mechanical properties of articular cartilage. In: Proceedings of the 47th Annual Meeting Orthopaedic Research Society. San Francisco, California.
Kokkonen, H.T., Makela, J., Kulmala, K.A., Rieppo, L., Jurvelin, J.S., Tiitu, V., et al., 2011. Computed tomography detects changes in contrast agent diffusion after collagen cross-linking typical to natural aging of articular cartilage. Osteoarthr. Cartil. 19 (10), 1190–1198.
Leddy, H.A., Guilak, F., 2008. Site-specific effects of compression on macromolecular diffusion in articular cartilage. Biophys. J. 95 (10), 4890–4895.
Loparic, M., Wirz, D., Daniels, A.U., Raiteri, R., Vanlandingham, M.R., Guex, G., Martin, I., Aebi, U., Stolz, M., 2010. Micro- and nanomechanical analysis of articular cartilage by indentation-type atomic force microscopy: validation with a gel-microfiber composite. Biophys. J. 98 (11), 2731–2740.
McGann, M.E., Bonitsky, C.M., Ovaert, T.C., Wagner, D.R., 2014. The effect of collagen crosslinking on the biphasic poroviscoelastic cartilage properties determined from a semi-automated microindentation protocol for stress relaxation. J. Mech. Behav. Biomed. Mater. 34, 264–272.
Moshtagh, P.R., Pouran, B., Korthagen, N.M., Zadpoor, A.A., Weinans, H., 2016a. Guidelines for an optimized indentation protocol for measurement of cartilage stiffness: the effects of spatial variation and indentation parameters. J. Biomech. 49 (14), 3602–3607.
Moshtagh, P.R., Pouran, B., van Tiel, J., Rauker, J., Zuiddam, M.R., Arbabi, V., et al., 2016b. Micro- and nano-mechanics of osteoarthritic cartilage: the effects of tonicity and disease severity. J. Mech. Behav. Biomed. Mater. 59, 561–571.
Notbohm, J., Poon, B., Ravichandran, G., 2011. Analysis of nanoindentation of soft materials with an atomic force microscope. J. Mater. Res. 27 (01), 229–237.
Oliver, W.C.P.G., 1992. An improved technique for determining hardness and elastic modulus using load and displacement sensing indentation experiments. Mater. Res. 7, 1564–1583.
Rauker, J., Moshtagh, P.R., Weinans, H., Zadpoor, A.A., 2014. Analytical relationships for nanoindentation-based estimation of mechanical properties of biomaterials. J. Mech. Med. Biol. 14 (03), 1430004.
Saudek, D.M., Kay, J., 2003. Advanced glycation end products and osteoarthritis. Curr. Rheumatol. Rep. 5 (1), 33–40.
Sophia Fox, A.J., Bedi, A., Rodeo, S.A., 2009. The basic science of articular cartilage: structure, composition, and function. Sports Health 1 (6), 461–468.
Stolz, M., Gottardi, R., Raiteri, R., Miot, S., Martin, I., Imer, R., Staufer, U., Raducanu, A., Duggelin, M., Baschong, W., Daniels, A.U., Friederich, N.F., Aszodi, A., Aebi, U., 2009. Early detection of aging cartilage and osteoarthritis in mice and patient samples using atomic force microscopy. Nat. Nanotechnol. 4 (3), 186–192.
Tomkoria, S., Patel, R.V., Mao, J.J., 2004. Heterogeneous nanomechanical properties of superficial and zonal regions of articular cartilage of the rabbit proximal radius condyle by atomic force microscopy. Med. Eng. Phys. 26 (10), 815–822.
Verzijl, N., DeGroot, J., Ben, Z.C., Brau-Benjamin, O., Maroudas, A., Bank, R.A., et al., 2002. Crosslinking by advanced glycation end products increases the stiffness of the collagen network in human articular cartilage: a possible mechanism through which age is a risk factor for osteoarthritis. Arthritis Rheum. 46 (1), 114–123.
Zadpoor, A.A., 2015. Nanomechanical characterization of heterogeneous and hierarchical biomaterials and tissues using nanoindentation: the role of finite mixture models. Mater. Sci. Eng. C. Mater. Biol. Appl. 48, 150–157.